Synthesis and Steric Stabilization of Silver Nanoparticles in Neat Carbon Dioxide Solvent Using Fluorine-Free Compounds

Madhu Anand, Philip W. Bell, Xin Fan,† Robert M. Enick,† and Christopher B. Roberts*

Department of Chemical Engineering, Auburn University, Auburn, Alabama 36849, and Department of Chemical Engineering, University of Pittsburgh, Pittsburgh, Pennsylvania 15261

Received: March 8, 2006; In Final Form: May 26, 2006

The adjustable solvent properties, vanishingly low surface tensions, and environmentally green characteristics of supercritical carbon dioxide present certain advantages in nanoparticles synthesis and processing. Unfortunately, most current techniques employed to synthesize and disperse nanoparticles in carbon dioxide use environmentally persistent fluorinated compounds as metal precursors and/or stabilizing ligands. This paper illustrates a one-step process for synthesis and stabilization of silver nanoparticles in carbon dioxide using only fluorine-free compounds. Isostearic acid coated silver nanoaparticles were formed and stably dispersed through arrested precipitation. Silver bis(3,5,5-trimethyl-1-hexyl)sulfosuccinate (Ag-AOT-TMH) was reduced in the presence of isostearic acid as a capping ligand in carbon dioxide solvent to form silver nanoparticles. The addition of cyclohexane as cosolvent or an increase in carbon dioxide solvent density enhances the dispersibility of the particles due to an increase in solvent strength. The dispersibility of the isostearic acid capped silver nanoparticles diminished with time until a stable dispersion was achieved due to the precipitation of a fraction of particle sizes too large to be stabilized by the solvent medium, thereby leaving a smaller size fraction of nanoparticles stably dispersed in the CO_2 mixtures. This paper presents the one-step synthesis and stabilization of metallic nanoparticles in neat carbon dioxide without the aid of any fluorinated compounds.

Introduction

Supercritical fluids (SCFs) have received a great deal of attention in the area of nanomaterial synthesis and processing due to their unique characteristics of tunable physicochemical properties, vanishingly low surface tensions, and excellent wetting properties. Physicochemical properties such as density, diffusivity, and solubility parameter can be readily altered by varying the pressure and temperature, creating opportunities for use in a number of processes.[1] Carbon dioxide (CO_2) is the most commonly used supercritical fluid because it is cheap, relatively inert, nontoxic, readily available, nonflammable, miscible with many organic liquids, and environmentally benign. In addition to these attributes, the critical temperature (304 K) and the critical pressure (73.8 bar) of CO_2 are easily accessible.

The unique tunable solvent properties of CO_2 have been successfully used in the controlled synthesis of metal nanoparticles using a variety of fluorinated precursors, ligands, and surfactants.[2−15] For example, Shah et al.[3] studied the effects of CO_2 density on the synthesis of perfluorodecanethiol-stabilized silver (Ag) nanoparticles in CO_2. They found that higher CO_2 densities yielded 2-nm Ag nanoparticles compared to 4-nm particles at lower CO_2 densities. The tunable solvent properties of supercritical fluids have also been used to control the size selective dispersion of nanoparticles. Shah et al.[16] demonstrated the size-selective dispersion of dodecanethiol-coated nanoparticles in supercritical ethane by density tuning, where the largest particle sizes were dispersed at the highest pressure and vice versa. CO_2 solvent systems also offer unique wetting characteristics that can be used to improve the deposition of metal films on surfaces[17,18] and the deposition of nanoparticles on surfaces into uniform monolayers.[19,20] McLeod et al.[19] and Shah et al.[20] used dispersions of nanoparticles in supercritical CO_2 and compressed liquid CO_2, respectively, in the formation of thin films of Ag nanoparticles with wider surface area coverage and uniformity compared to the films obtained by simple solvent-evaporation techniques. While CO_2 does offer certain processing advantages (e.g. tunable solvent strength and wetting characteristics), its use in nanoparticle synthesis, dispersion, and processing is limited by the current need for fluorinated compounds resulting from its relatively poor solvent strength.

CO_2 is a feeble solvent because of its very low dielectric constant (1.1−1.5) and zero dipole moment, resulting in low solubility of many organic species. The very low polarizability per unit volume and low refractive index of CO_2 results in weaker van der Waals forces than hydrocarbon solvents, making CO_2 more similar to fluorocarbons with respect to solvent strength.[21] Fluorinated surfactants[22] have shown high solubility in CO_2 and some of them have stabilized water in CO_2 microemulsions.[21,23] Nanoparticles have been formed in CO_2 within water in CO_2 (W/C) microemulsions or by arrested precipitation techniques using fluorinated compounds. Shah et al.[24] has written a descriptive review on nanoparticle synthesis and dispersibility in supercritical fluids. Both fluorinated surfactants and fluorinated ligands have been used to disperse particles in CO_2. Interactions between the CO_2 solvent and the fluorinated coating on the nanoparticles provide enough repulsive forces to counterbalance the attractive van der Waals forces between the particles. In W/C microemulsion systems, fluori-

* Corresponding author. Phone: (334) 844-2036. Fax: (334) 844-2063. E-mail: croberts@eng.auburn.edu.
† University of Pittsburgh.

10.1021/jp0614401 CCC: $33.50
Published on Web 07/13/2006

nated surfactant supported aqueous cores act as nanoreactors to synthesize and then disperse the particles in a CO_2 phase due to strong interactions between CO_2 and the fluorinated surfactant tails. Various types of particles have been prepared in W/C microemulsions, including Ag,[8,12] Ag halide,[13] Cu,[7] and semiconductor[11] nanoparticles. Because fluorinated compounds are environmentally persistent and expensive, researchers are also trying to develop CO_2-philic fluorine-free compounds or surfactants to form stable microemulsions in CO_2. For nonfluorinated compounds, the disadvantages of poor solubilities and high cloud point pressures can be overcome by adding cosolvents or CO_2-philic compounds. These cosolvents interact more strongly with the solute than does CO_2 and can increase the solubility. Zhang et al.[25] produced Au nanoparticles in CO_2-induced reverse micelles of nonfluorinated surfactants using a mixture of *p*-xylene and CO_2. One class of compounds that have shown high solubility in CO_2 are highly branched, methylated, and stubby surfactants due to increased tail solvation and weak tail−tail interactions.[26−29] Researchers utilized stubby hydrocarbon surfactants,[30,31] ionic hydrocarbon surfactants,[32,33] and trisiloxane surfactants[26] to stabilize both microemulsions and macroemulsions in CO_2.

Nanoparticles have also been synthesized in supercritical CO_2 using arrested precipitation techniques where the particles are dispersed in a single continuous CO_2 phase while the aqueous phase is eliminated. Arrested precipitation is one of the most successful solution-based techniques for nanoparticle synthesis in conventional solvents. In this technique, an organometallic precursor soluble in a given solvent is reduced in the presence of a capping ligand[34] used to stabilize the particle and to quench further growth. Shah[3,4] and Mcleod[9] used this technique in supercritical CO_2 and capped the synthesized nanoparticles with fluorinated thiol stabilizing ligands. Recently, Fan[10] was also successful in using a nonfluorinated precursor silver bis(3,5,5-trimethyl-1-hexyl)sulfosuccinate (Ag-AOT-TMH) and fluorinated thiols to stably disperse the particles in CO_2. They used a nonfluorinated organometallic compound, Ag-AOT-TMH, a highly methylated stubby compound with very high solubility in CO_2, but fluorinated ligands were still used. Even though fluorinated compounds generally have higher solubility in CO_2, the cost and environmental problems of fluorinated compounds present drawbacks to their use in many processing applications.

Recently, Bell et al.[35] used a stubby nonfluorinated compound, isostearic acid, to disperse Ag nanoparticles in compressed liquid CO_2. In this technique, nanoparticles were first made in a conventional organic solvent using sodium bis(2-ethylhexyl) sulfosuccinate (AOT) reverse micelles and then the capping agent was replaced by isostearic acid via ligand exchange. When these isostearic acid capped particles were introduced into CO_2, only a very small fraction of the synthesized particles were dispersed in CO_2, due to the difference between the solvent strength of CO_2 and the organic solvent in which the particles were synthesized.

This paper presents the synthesis and subsequent stable dispersion of metal nanoparticles in neat CO_2 solvent without the use of any fluorinated compounds. The process described herein utilizes nonfluorinated isostearic acid as a nanoparticle stabilizing ligand and Ag-AOT-TMH as a nonfluorinated metal precursor, where the whole process of Ag nanoparticle synthesis and dispersion is reduced to one step in neat CO_2 solvent. Cyclohexane was examined as a nonfluorinated cosolvent to further enhance the solvent strength of the CO_2 mixtures and hence the dispersibility of the isostearic acid capped nanoparticles.

Experimental Section

Materials. Silver nitrate (99.8%) was purchased from Acros. Isostearic acid (100%) was received from Nissan Chemical America Corp. Sodium bis(3,5,5-trimethyl-1-hexyl)sulfosuccinate (AOT-TMH) was provided by Julian Eastoe of the University of Bristol. Cyclohexane (99.5%) and hexane (99+%) were obtained from Aldrich. Sodium borohydride ($NaBH_4$) (ReagentPlus, 99%) and anhydrous ether (99+%) were acquired from Sigma. Ethanol (200 proof) was obtained from Florida Distillers. Deionized water used in the Ag-AOT-TMH synthesis was obtained from Fisher Scientific. Carbon dioxide (SFC/SFE grade) was obtained from Airgas. All materials were used as received.

Ag-AOT-TMH Synthesis. The CO_2-soluble silver salt, Ag-AOT-TMH, was synthesized by an ion-exchange of the AOT-TMH compound. The AOT-TMH synthesis has been described elsewhere.[36] The technique followed for the ion exchange was adapted from that given by Fan et al.[10] The procedure is briefly described here. $AgNO_3$ (5.025 g, 29.58 mmol) was dissolved in 10 mL of deionized water and AOT-TMH (0.8297 g, 1.8 mmol) was dissolved in 5 mL of ethanol. The two solutions were mixed for 6 h, and 6 mL of ether was added to form two phases. The two phases were separated, and the upper phase containing Ag-AOT-TMH was dried in a vacuum oven at room temperature. The remaining solid was redissolved in isooctane and centrifuged to remove any solid contaminants. The solid dissolved in isooctane was again dried in a vacuum oven at room temperature, resulting in a yellowish-brown solid, Ag-AOT-TMH.

Ag Nanoparticle Synthesis in CO_2. Ag-AOT-TMH was directly reduced in dense CO_2 to produce silver nanoparticles that were capped with isostearic acid ligands. The particle synthesis experiments were initiated by loading 0.0516 g of Ag-AOT-TMH (0.06 wt %); 0.175 g of isostearic acid (0.19 wt %); either 0, 2, or 10 mL of cyclohexane cosolvent; and a Teflon-coated magnetic stir bar into a 96-mL stainless steel vessel equipped with opposing quartz windows to allow passage of a UV−vis beam. The vessel was then pressurized with CO_2 to 207 bar at 295 K. The contents were stirred for 1 h to fully dissolve all solutes and achieve a single-phase mixture. Then 540 μL of a 0.8 M $NaBH_4$ in ethanol solution was added using a six-port injection valve. The reducing agent was forced in by additional CO_2, increasing the total pressure to 276 bar. The silver nanoparticles formed by the reduction were monitored with UV−vis spectroscopy on a Varian 300E spectrophotometer. The vessel was depressurized and the particles were collected from the bottom of the vessel in hexane.

Ag Nanoparticle Imaging. A Zeiss EM 10 transmission electron microscope (TEM) was used to image the particles. TEM grids of the particles that were dispersed in CO_2 were prepared by directly spraying the CO_2 nanoparticle dispersion from the high-pressure cell through a needle valve onto a carbon-coated TEM grid. Once the TEM grids of the dispersed particles were collected through this spray technique, the vessel was completely depressurized as described in the section above to allow precipitation of the dispersed particles. A small amount of hexane was then added to the vessel to redisperse all of the particles synthesized. To analyze all of the particles synthesized in CO_2 (both those that were dispersed in CO_2 and those that were not), a TEM grid was prepared by evaporating the hexane from a droplet of dispersion collected from the bottom of the vessel directly on a carbon-coated copper grid. Sizing of the silver nanoparticles from the TEM images was performed using ImageJ software, where each particle was bounded by a

rectangle and the diameter was approximated by the average of the length and width.

Infrared Spectroscopy of Ag Nanoparticles. Fourier transform infrared (FTIR) spectroscopy was performed using a Nicolet Avatar 360 FT-IR spectrometer to investigate the nature of the chemical interaction between the isostearic acid ligands and the silver nanoparticles. The resolution used was 2 cm^{-1} and the number of scans was 64.

To prepare the nanoparticles for FTIR analysis, the hexane nanoparticle dispersion obtained after the depressurization of the vessel was mixed with ethanol as an antisolvent. The dispersion of nanoparticles in the solvent/antisolvent mixture was then centrifuged (Fisher Centrific Model 228) to precipitate out the Ag nanoparticles. The particles were again washed with ethanol and centrifuged to remove any free isostearic acid molecules from the precipitate. This process of washing with ethanol was repeated three times, and then the silver particles were dried in an oven (>60 °C) under vacuum overnight. Finally, to obtain the transmission spectra, pellets were made by mixing these particles (1 mg) with KBr powder (100 mg).

Results and Discussion

Ag Nanoparticle Synthesis and Stabilization in Neat CO_2. Ag-AOT-TMH and isostearic acid, shown in Figure 1, were chosen as silver organometallic precursor and stabilizing ligand, respectively, for the synthesis and subsequent dispersion of silver nanoparticles in CO_2, due to their highly methylated, branched tails. Values from the pressure−composition diagram for the Ag-AOT-TMH−CO_2 mixture[10] and isostearic acid−CO_2 mixture[35] obtained through phase behavior measurements demonstrate that these compounds are highly soluble in CO_2. The branched, methylated tails in these compounds result in effective CO_2−tail solvation and weak tail−tail interactions.[27,35,37] These effects lead to high CO_2 solubility. Isostearic acid is completely miscible with CO_2 at pressures above 138 bar at 295 K, as shown in the phase behavior studies done by Bell et al.[35]

AOT-TMH and Ag-AOT-TMH have similar solubilities[10] in CO_2 because the only difference between the two structures is a change in the cation. These compounds are soluble in dense CO_2 because of the branched methylated tails, and as expected, the cloud point pressure at low weight percentages is low. This phase behavior data was collected at 313 K, while our experiments were conducted at 295 K. Figure 1 in the Supporting Information shows that the cloud point pressure decreases with a decrease in temperature for AOT-TMH. The phase behavior experiments at different temperatures were not performed for Ag-AOT-TMH due to the limited quantity of material available. Due to the similarity between the structure of the two surfactants and their phase behavior data, it is expected that less pressure is required to dissolve Ag-AOT-TMH at 295 K than 313 K. It is clear from the phase behavior studies for Ag-AOT-TMH performed by Fan et al.[10] that less than 100 bar is required to dissolve the 0.06 wt % Ag-AOT-TMH used in our experiments at 313 K. To dissolve the solid, the vessel was pressurized to 206 bar at 295 K. No solid was observed in the vessel after mixing, and silver nanoparticles were formed, indicating that the Ag-AOT-TMH was sufficiently soluble in CO_2 under the experimental conditions used.

The one-step process for synthesis and stabilization of silver nanoparticles in pure CO_2 takes advantage of the solubility of Ag-AOT-TMH and isostearic acid in CO_2. The UV−vis absorbance spectrum for silver nanoparticles synthesized in pure CO_2 is shown in Figure 2. The absorbance band centered at a wavelength of 419 nm is attributed to the absorption of silver

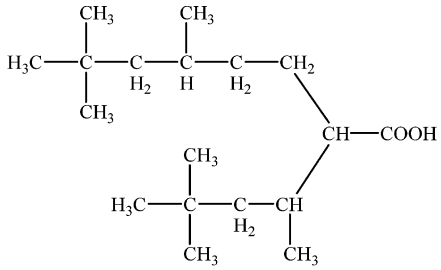

Iso-Stearic Carboxylic Acid, $C_{17}H_{35}COOH$ (Mn=284g/mol)

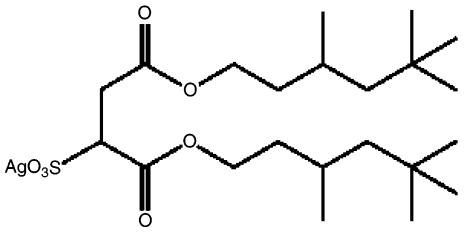

Figure 1. (a) Molecular structure of isostearic acid.[35] (b) Molecular structure of Ag-AOT-TMH.[10]

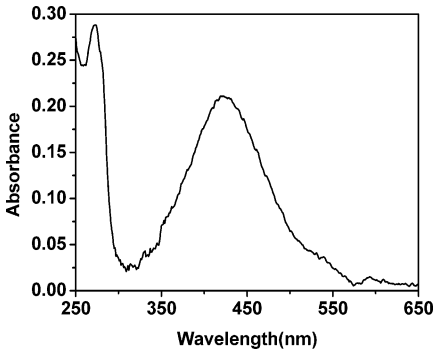

Figure 2. UV−vis absorbance spectrum of isostearic acid coated Ag nanoparticles synthesized and successfully dispersed in neat CO_2 collected after 3 days at 295 K and 276 bar.

nanoparticles dispersed in neat CO_2.[38] A single distinct absorption band in this wavelength range reflects the presence of spherically shaped silver particles. The UV−vis absorbance in this range is due to the excitation of plasmon resonances or interband transitions. This absorbance band decreased with time as the larger particles were unable to remain dispersed in the pure CO_2 phase. After 3 days, the absorbance ceased to change, indicating a stable dispersion of silver nanoparticles. The fraction of particles that remain dispersed after 3 days can be roughly estimated from the decrease in the intensity of the UV−vis absorbance band, since absorbance is proportional to the particle concentration in solution. On the basis of this rough estimate, 23% of the particles remained dispersed after 3 days. The effect of time on the absorption intensities of the nanoparticle dispersions is discussed in detail later in this paper. Figure 3 shows a TEM image of the silver nanoparticles synthesized in neat CO_2. Samples of these particles were prepared using both of the collection methods described above. Figure 3a shows a TEM image of particles synthesized in pure CO_2 that were collected from the bottom of the vessel after 3 days by depressurizing the vessel and subsequent redispersion in hexane solvent for grid preparation (this sample includes both particles that were dispersed in CO_2 and those that were not). Figure 3b shows a TEM image of particles synthesized and successfully dispersed in pure CO_2 at 295 K and 276 bar. This sample was collected 3 days after synthesis by simply spraying the CO_2 nanoparticle dispersion directly onto a TEM grid surface. These

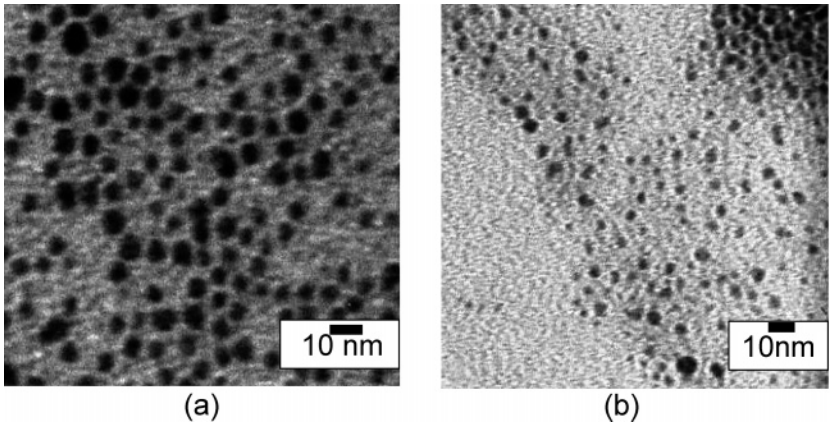

Figure 3. TEM images of isostearic acid coated silver nanoparticles synthesized in pure CO_2 at 295 K and 276 bar. (a) Particles recovered from the bottom of the vessel after 3 days by depressurizing the vessel and subsequent redispersion in hexane solvent for grid preparation. This sample includes both particles that were dispersed in CO_2 and those that were not. (b) Particles collected 3 days after synthesis by simply spraying the CO_2 nanoparticle dispersion directly onto a TEM grid surface. This sample shows a TEM image of particles synthesized and successfully dispersed in CO_2.

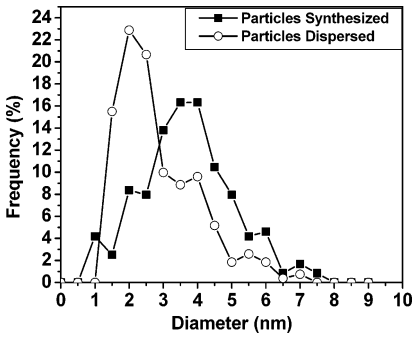

Figure 4. Size distributions of isostearic coated Ag nanoparticles (■) synthesized or (○) synthesized and successfully dispersed in pure CO_2 at 276 bar and 295 K.

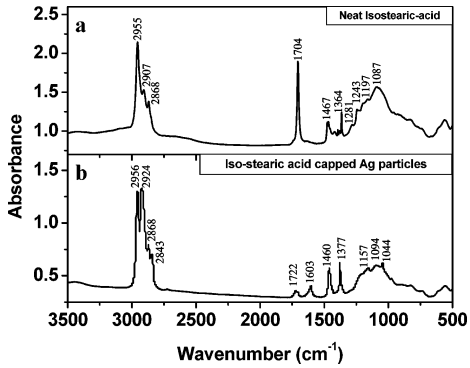

Figure 5. FTIR spectra of (a) neat isostearic acid and (b) isostearic acid coated silver nanoparticles.

images clearly illustrate that Ag nanoparticles can be synthesized and stabilized in neat CO_2 without the need for fluorinated ligands. It is clear from these images that only the smaller fraction of particles synthesized could be dispersed in CO_2. Figure 4 presents the size distributions of the particles obtained using both collection methods. The average size and standard deviation of the particles synthesized in pure CO_2 (collected on the bottom of the vessel after depressurization) are 3.4 nm and ±1.3 nm (relative standard deviation 39%), respectively. On the other hand, the average size and standard deviation of the particles synthesized and then dispersed in CO_2 (collected from spray process) are 2.6 nm and ±1.2 nm (relative standard deviation 45%), respectively. While larger particles were formed in the synthesis and subsequent growth process in CO_2, only the smallest particles were sufficiently solvated by the CO_2 solvent to be stably dispersed. This was also illustrated by a decrease in the magnitude of the UV−vis absorbance peak as the larger fraction of particles precipitated over time, as discussed later in this paper. These results demonstrate the successful synthesis and dispersion of metallic nanoparticles in pure CO_2 without the use of any fluorinated compounds. Additionally, no organic solvents were required during the synthesis or dispersion.

Infrared Spectroscopy of Isostearic Acid Coated Ag Nanoparticles. FTIR spectroscopy analysis was performed to verify the presence of the acid on the surface of the Ag nanoparticles and to study the nature of the adsorption of the capping material on the silver nanoparticles surface. Figure 5 shows the FTIR spectrum of (a) neat isostearic acid and (b) Ag nanoparticles capped with isostearic acid as synthesized in CO_2. These particles were collected in hexane after depressurizing the high-pressure vessel and further washed with ethanol to remove any free isostearic acid using the washing process described in the Experimental Section above. Figure 5a shows the FTIR spectra of neat isostearic acid, where the broad band between 3400 and 2500 cm^{-1} corresponds to the O−H stretch of the carboxylic acid.[39] Bands superimposed on the O−H stretch correspond to the asymmetric (2955 cm^{-1}) and symmetric (2868 cm^{-1}) CH_2 stretch, respectively.[40] The peak at 1704 cm^{-1} corresponds to the C═O stretch. Carboxylic acids (COOH) typically have a characteristic C═O stretching vibration at ∼1750 cm^{-1}; however, extensive hydrogen bonding in the liquid state between the hydroxyl and carbonyl groups can lower the frequency corresponding to the C═O stretch to ∼1700 cm^{-1}.[41] Figure 5b corresponds to the FTIR spectrum of Ag nanoparticles coated with isostearic acid. Slight shifts were observed for the CH_2 stretches toward the lower frequencies, indicating that the adsorbed hydrocarbon chains on the silver nanoparticles are in a close-packed, crystalline state. [40] The carbonyl stretch has shifted to 1722 cm^{-1}, which represents a significant shift (∼30 cm^{-1}) compared to the acid (∼1750 cm^{-1}). This blue shift can be due to the bonding between the hydroxyl oxygen and the silver metal surface, resulting in the C═O bond having less electron density and therefore causing a frequency shift.[41] El-Sayed and co-workers have referred to this bonding as an ester-like linkage between the capping material and the nanoparticle surface.[41] A new peak at 1603 cm^{-1} that is characteristic of the carboxylate asymmetric stretch ($COO^-_{(a)}$) was also present in the FTIR spectrum of the isostearic acid capped particles.[42] The region between 1377 and 1460 cm^{-1} results from the

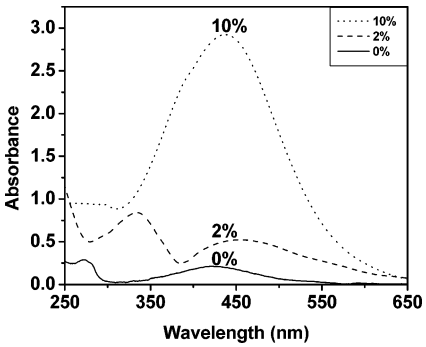

Figure 6. UV−vis absorbance spectra of isostearic acid coated Ag nanoparticles synthesized and dispersed in CO_2 with 0, 2, and 10% cyclohexane cosolvent by volume at 295 K and 276 bar. The dotted line corresponds to the UV−vis absorbance spectrum collected 5 days after silver nanoparticles were synthesized in CO_2 with 10% cyclohexane cosolvent by volume, the dashed line corresponds to the UV−vis absorbance spectrum collected 3 days after particles were synthesized with 2% cyclohexane cosolvent by volume, and the solid line corresponds to the UV−vis absorbance spectrum collected 3 days after silver nanoparticles were synthesized in pure CO_2. These UV−vis absorbance spectra were acquired after each system had reached a stable dispersion. The spectra have been scaled to have an absorbance of 0 at 700 nm for comparison.

backbone vibrations (CH_2 deformation and wagging) overlapping with the symmetric vibration ($COO^-_{(s)}$).[41] It is well-known from the literature on IR data for surface carboxylate bonding that there may exist two types of binding when the carboxylate ion coordinates to a metal.[43] In one of the binding types, the carboxylate is connected symmetrically with equivalent oxygen atoms to the surface of the metal and only the symmetric stretch ($COO^-_{(s)}$) is present.[44] But, in the other binding type, the carboxylate is connected to the metal through only one oxygen atom and both the symmetric ($COO^-_{(s)}$) as well as asymmetric ($COO^-_{(a)}$) stretches were observed.[45] Wu et al. has also mentioned that when the carboxylate is chemisorbed on the metal surface through inequivalent oxygen atoms, then a C═O band (1700−1730 cm^{-1}) is still present.[40] The decrease in intensity of the C═O band in the spectrum for the isostearic acid capped particles compared to the spectrum for the isostearic acid further verifies the formation of the bond.[41] The symmetric ($COO^-_{(s)}$) and asymmetric ($COO^-_{(a)}$) stretches as well as the carbonyl stretch is present in the FTIR spectrum of the isostearic acid capped silver particles. This suggests that isostearic acid is connected to the Ag particles through one oxygen atom.

Effect of Cosolvent on Ag Nanoparticle Dispersion in CO_2. The addition of organic cosolvents can have a significant impact on nanoparticle dispersion in CO_2 solvent systems. While dodecanethiol-coated silver nanocrytals could not be dispersed in supercritical CO_2 alone, Shah et al.[5] found that they were able to disperse dodecanethiol-coated silver nanocrystals by adding 50% (volume fraction) hexane as cosolvent. Recently, Anand et al.[46] showed that solvent strength in various CO_2/cosolvent mixtures has a significant impact on dodecanethiol-coated Au nanoparticle dispersibility, where an increase in the alkyl tail length of the cosolvent increased dispersibility. Cyclohexane has been shown to have stronger interactions with hydrocarbon ligand tails than other alkane solvents, allowing larger sized metallic nanoparticles to be dispersed in both liquid and supercritical solvent/cosolvent systems.[47−49]

Cyclohexane was examined as a cosolvent in the synthesis of isostearic acid coated silver nanoparticles in CO_2 in an effort to increase dispersibility without the addition of fluorinated compounds. Figure 6 shows a comparison of the UV−vis absorbance spectra of isostearic acid coated Ag nanoparticles synthesized and dispersed in CO_2 with 0, 2, and 10% cyclohexane cosolvent by volume at 295 K and 276 bar. The dotted line corresponds to the UV−vis absorbance spectrum collected 5 days after silver nanoparticles were synthesized in CO_2 with 10% cyclohexane cosolvent by volume, the dashed line corresponds to the UV−vis absorbance spectrum collected 3 days after particles were synthesized with 2% cyclohexane cosolvent by volume, and the solid line corresponds to the UV−vis absorbance spectrum collected 3 days after silver nanoparticles were synthesized in pure CO_2. These UV−vis absorbance spectra were acquired after each system had reached a stable dispersion. Although a stable dispersion of silver nanoparticles was obtained in pure CO_2, the addition of a small amount of cyclohexane cosolvent (up to 10 vol %) significantly enhanced the concentration of dispersed isostearic acid coated silver nanoparticles in CO_2. Cyclohexane solvates the ligand tails much better than does CO_2, greatly increasing the solvent strength, and consequently the number of particles that can be stably dispersed in the mixture. These results indicate that the interactions between the isostearic acid ligand tails and the alkane cosolvent play a critical role in the dispersion of nanoparticles in CO_2. A disadvantage to using alkane cosolvents to increase the dispersibility of these nanoparticles, on the other hand, is that the critical point of the mixture is increased above that of pure CO_2. Therefore, a higher temperature is required to operate within the critical regime of the mixture to take full advantage of the unique properties that supercritical solvents offer in nanomaterial processing.

The UV−vis absorbance spectrum of the isostearic acid coated Ag nanoparticles dispersed in CO_2 with 10% cyclohexane cosolvent has a single absorbance band centered at 437 nm, indicating the presence of spherical silver nanoparticles. The UV−vis spectra of the nanoparticle dispersions in CO_2 with 2 and 0% cyclohexane cosolvent, on the other hand, have multiple absorbance bands. These multiple absorption bands have been attributed to the stabilization of silver nanoparticle intermediates and silver clusters composed of small numbers of atoms.[8] For example, the UV−vis spectrum for the 2% cyclohexane system has absorbance bands at 250, 340, and 450 nm. The band at 250 nm corresponds to the presences of Ag_4^{2+},[8,50] whereas the band at 340 nm may be attributed to a wider range of intermediates, including metal silver atom (Ag^0) and its oligomeric clusters[51] including Ag_9^+ and Ag_8^{2+}.[52] These oligomeric clusters could then proceed to the formation of colloidal metallic silver nanoparticles, as indicated by the band at 450 nm. Metallic silver nanoparticles are commonly characterized by an absorption in the range of 400−450 nm, depending upon the size, shape, and surrounding environment in which the nanoparticle is situated.[38,50,53] Similarly for 0% cyclohexane, the absorbance bands at 273 and 419 nm show the presence of Ag_4^{2+} intermediates and silver nanoparticles, respectively. The addition of 10% cyclohexane causes a diminution of the absorbance bands corresponding to silver intermediates and results in a single absorbance band at 437 nm, indicative of stabilized silver nanoparticles.

TEM images of the particles synthesized in CO_2 using 0, 2, and 10% cyclohexane cosolvent are shown in Figure 7. Samples of these particles were again prepared using both of the collection methods described above. Figure 7i presents TEM images of isostearic acid coated Ag nanoparticles synthesized and successfully dispersed in the CO_2/cyclohexane mixtures at 295 K and 276 bar, where the samples were collected 24 h after synthesis by simply spraying the CO_2 nanoparticle dispersions directly onto a TEM grid surface. Figure 7ii shows TEM images

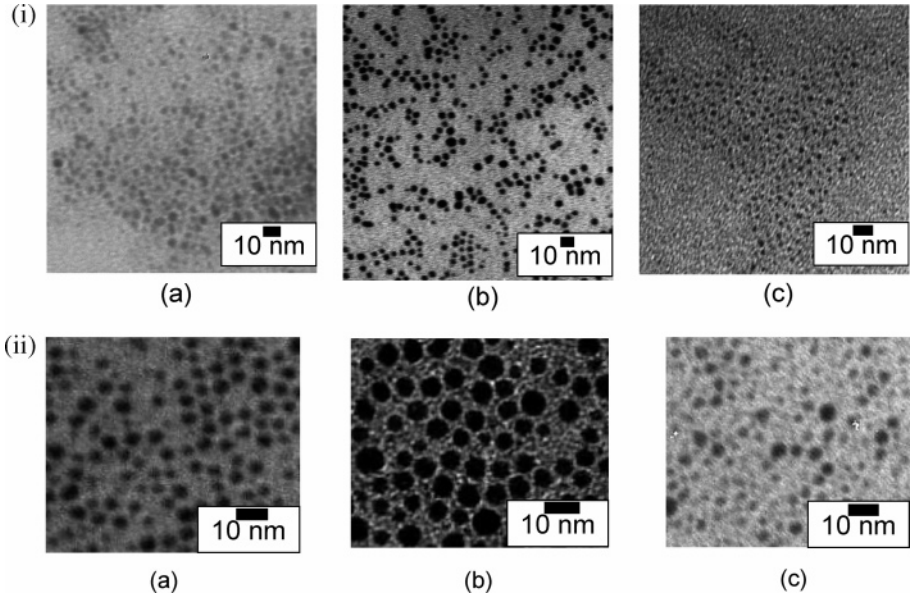

Figure 7. (i) TEM images of isostearic acid coated silver nanoparticles synthesized and successfully dispersed in the CO_2/cyclohexane mixtures at 295 K and 276 bar with (a) no cosolvent, (b) 2% cyclohexane, and (c) 10% cyclohexane. These particles were collected 24 h after synthesis by spraying the CO_2 nanoparticle dispersions directly onto a TEM grid surface. (ii) TEM images of isostearic acid coated silver nanoparticles synthesized in the CO_2/cyclohexane mixtures at 295 K and 276 bar with (a) no cosolvent, (b) 2% cyclohexane, and (c) 10% cyclohexane. These samples include both particles that were dispersed in the CO_2/cyclohexane mixtures as well as those that were not dispersed after synthesis. These particles were recovered from the bottom of the vessel in hexane after depressurizing the vessel. The hexane dispersion was then allowed to evaporate on the TEM grid.

of the particles collected from the bottom of the vessel by depressurizing the vessel and subsequently redispersing the particles in hexane solvent for grid preparation. Please note that these samples include both particles that were dispersed in the CO_2/cyclohexane mixtures as well as those that were not dispersed after synthesis. These particles shown in Figure 7ii were collected after stable dispersions were achieved (3 days for 0 and 2% cyclohexane and 5 days for 10% cyclohexane), as indicated by the unvarying UV−vis absorption spectra in the CO_2/cyclohexane mixtures. The TEM images in Figure 7i,ii indicate that, while a range of particle sizes could be synthesized in the CO_2/cyclohexane mixtures, only the smaller particles could be dispersed in the CO_2/cyclohexane mixtures after more than 24 h. The particles that were synthesized at each cyclohexane concentration in CO_2 shown in Figure 7ii were larger in each case than the particles dispersed at the corresponding CO_2/cyclohexane mixture shown in Figure 7i. This signifies that even the addition of 10% (volume fraction) cyclohexane as a cosolvent in the CO_2/cyclohexane mixture did not provide enough solvent strength to stabilize all of the synthesized particles. Moreover, it is also visible from these pictures that particles synthesized in CO_2 with 2% volume fraction of cyclohexane are bigger than the particles synthesized in pure CO_2, but further addition of cyclohexane to 10 vol % has an adverse effect on particle size determined from both collection techniques shown in Figure 7i,ii. Figure 8a presents the particles size distributions of the isostearic acid coated silver nanoparticles that were both synthesized and successfully dispersed in each of the CO_2/cyclohexane mixtures at 295 K and 276 bar. The average size of the particles synthesized and then dispersed in pure CO_2 (collected from the spray process) as mentioned in an earlier section is 2.6 nm. With the addition of 2% (vol) cyclohexane to CO_2, the mean particle size increases to 3.4 nm, an increase of almost 0.8 nm. Interestingly, with the further addition of cyclohexane to 10 vol % in CO_2, the mean particle size decreases to 1.6 nm. Similar trends were observed from the particles collected after depressurization. Figure 8b presents

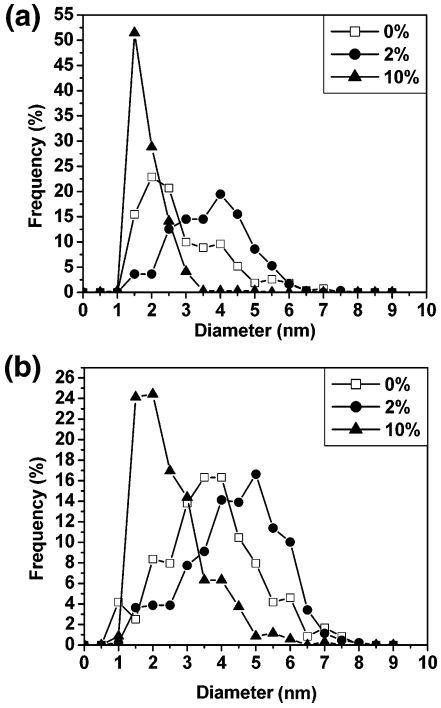

Figure 8. (a) Size distribution of isostearic acid coated silver nanoparticles synthesized and dispersed in CO_2 at 295 K and 276 bar with (□) no cosolvent, (●) 2% cyclohexane, and (▲) 10% cyclohexane. These particles were collected 24 h after synthesis by spraying the CO_2 nanoparticle dispersions directly onto a TEM grid surface. (b) Size distribution of isostearic acid coated silver nanoparticles synthesized in CO_2 at 295 K and 276 bar with (□) no cosolvent, (●) 2% cyclohexane, and (▲) 10% cyclohexane. These particles were recovered from the bottom of the vessel in hexane after depressurizing the vessel, and then the hexane dispersion was allowed to evaporate on the TEM grid. These samples include both particles that were dispersed in the CO_2/cyclohexane mixtures as well as those that were not dispersed after synthesis.

the size distributions of the isostearic acid coated silver particles (both those that were dispersed in the mixture and those that

were not) in each of the CO_2/cyclohexane mixtures at 295 K and 276 bar. The average size of the particles synthesized in pure CO_2 (collected from the bottom of the vessel after depressurization) is 3.4 nm, and this size is larger than the particles that were actually dispersed (2.6 nm), indicating that the CO_2 solvent was only able to disperse a smaller size fraction of the particles that were synthesized. The addition of 2% cyclohexane to CO_2 increases the mean particle size to 4.2 nm, again a difference of 0.8 nm. For 10% cyclohexane in the CO_2/cyclohexane mixture, the size of the particles synthesized was reduced to 2.3 nm. In each of the CO_2/cyclohexane mixtures, the synthesized particles are larger than those that were successfully dispersed. Interestingly, the mean particle size did not increase monotonically with an increase in mixture solvent strength through the addition of the cosolvent (as observed in both means of particle collection). There seems to be an optimum amount of cyclohexane that would need to be added, between 0 and 10 vol %, to synthesize and/or disperse larger particles. Shah et al.[3] showed that good solvent conditions quenched the growth of silver nanocrystals in CO_2 in the presence of fluorinated thiols, resulting in smaller nanocrystals than those synthesized under poor solvent conditions (lower densities). In this case, perfluorodecanethiol-stabilized silver nanocrystals were synthesized in supercritical CO_2 via hydrogen reduction of silver acetylacetonate. It was found that, at earlier stages in the growth process, metal core coagulation competes with thiol ligand adsorption. Under poor solvent conditions, particles grew to larger sizes (4 nm at $P < 250$ bar, $T = 80$ °C compared to 2 nm at $P > 250$ bar, $T = 80$ °C) before the coverage of capping ligand was sufficient to prevent coagulation of the metal particles, illustrating a tunability of the particle sizes that could be synthesized through variations in solvent strength. On the other hand, Kitchens et al.[47,48] examined the effects of solvent strength on the synthesis of copper nanoparticles within (AOT) reverse micelles in liquid and compressed alkane systems. In this case, the AOT surfactant molecule more weakly adsorbs to the metal nanoparticle surface than a fluorinated thiol counterpart and hence prevents coagulation to a lesser extent. With the use of AOT as a capping agent, particles that are larger than 8 nm in size were synthesized and sterically stabilized in these liquid and compressed alkane systems. For example, the mean size of copper nanoparticles synthesized within AOT reverse micelles was increased from 8.6 to 12.6 nm by changing the solvent from pentane to cyclohexane, where cyclohexane better solvates the AOT surfactant tails. Similarly, an increase in the solvent strength by tuning the pressure from 400 to 550 bar resulted in an increase in copper nanoparticle size from 8.6 to 9.3 nm in compressed ethane solvent at 20 °C. These examples illustrate that several factors can influence the particle size that can be synthesized and sterically stabilized in solution, including particle−particle interactions, the ligand adsorption on the metal nanoparticle, and the solvation of the ligand by the solvent medium.

Effect of Pressure on Ag Nanoparticle Dispersion in CO_2. Another factor that was examined was the effect of pressure (or density) at constant temperature on the dispersability of isostearic acid coated Ag nanoparticles formed by reduction in CO_2/cyclohexane mixtures. Shah et al.[16] varied the dispersability of dodecanethiol-stabilized gold and silver nanoparticles in liquid and supercritical ethane by altering the pressure and thereby tuning the solvent density. They were able to increase the particle dispersibility at higher pressure due to an increase in solvent density. Saunders et al.[6] performed small-angle X-ray scattering (SAXS) studies on interparticle interactions between perfluoropolyether (PFPE) coated gold nanocrystals in $scCO_2$. They observed an increase in interparticle attraction and, hence, particle aggregation at lower CO_2 density, which indicates that particle dispersability is a strong function of solvent density.

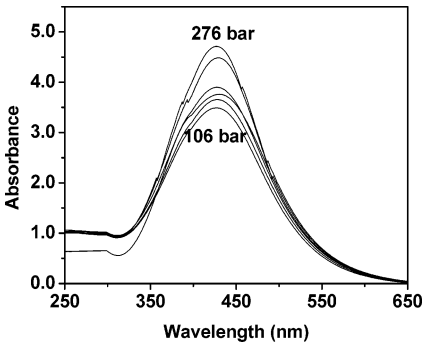

Figure 9. UV−vis absorbance spectra for isostearic acid coated silver nanoparticles dispersed in CO_2 at 295 K and various CO_2 pressures with 10% cyclohexane cosolvent by volume. Each curve corresponds to a different pressure going from the bottom curve (106 bar) to the top curve (276 bar). The spectra have been scaled to have an absorbance of 0 at 700 nm for comparison.

UV−vis absorbance spectra for dispersions of isostearic acid coated silver nanoparticles at different pressures (or densities) at 295 K are shown in Figure 9. These particles were synthesized by reduction of Ag-AOT-TMH in CO_2 with 10% cyclohexane cosolvent by volume at 295 K and 276 bar. This system was chosen because it had the largest concentration of dispersed particles, making changes in the concentration of dispersed particles easier to distinguish. After particle synthesis at 295 K and 276 bar, the high-pressure vessel was depressurized to 106 bar (0.10 g/mL). Once a stable dispersion was achieved, the pressure (or density) of the mixture was then increased by adding more CO_2. At each pressure, the system was given enough time for the UV−vis absorbance to not change appreciably. This time was typically less than 1 h. The UV−vis absorbance was then recorded and the pressure was increased. This process was repeated for six pressures until the mixture was returned to the initial condition of 276 bar (0.96 g/mL). As the pressure (or density) of the system was increased, the absorbance peak also increased, presumably resulting from the redispersion of the larger particles that had precipitated once the pressure was reduced to 106 bar. This increase in absorbance corresponds to an increase in the concentration of dispersed particles with an increase in density. By increasing the density at a constant temperature, the solvent strength of the system improves as CO_2 more effectively solvates the isostearic acid ligand tails and hence has the capacity to disperse larger particles that add to the concentration of dispersed particles in solution.

Effect of Temperature on Ag Nanoparticle Dispersion in CO_2. The results presented to this point involve nanoparticle dispersions in liquid-phase CO_2 at 295 K and 276 bar. To harness the full potential of the processing advantages that CO_2 can offer (e.g., high diffusivities and low surface tensions) it is necessary to retain the Ag nanoparticle dispersions under supercritical CO_2 conditions at elevated temperatures. Once a stable dispersion of nanoparticles was produced in neat CO_2 at 295 K and 276 bar, the temperature of the system was sequentially increased from 295K to 298, 303, and 308 K at a constant density of 0.96 g/mL and held at each of these temperatures for 1 h. No change was observed in the UV−vis absorbance spectrum with these sequential changes in temperature (data not shown). Since there was no observable change in the UV−vis absorbance spectra at these different temperatures with constant CO_2 density, the silver nanoparticles can therefore

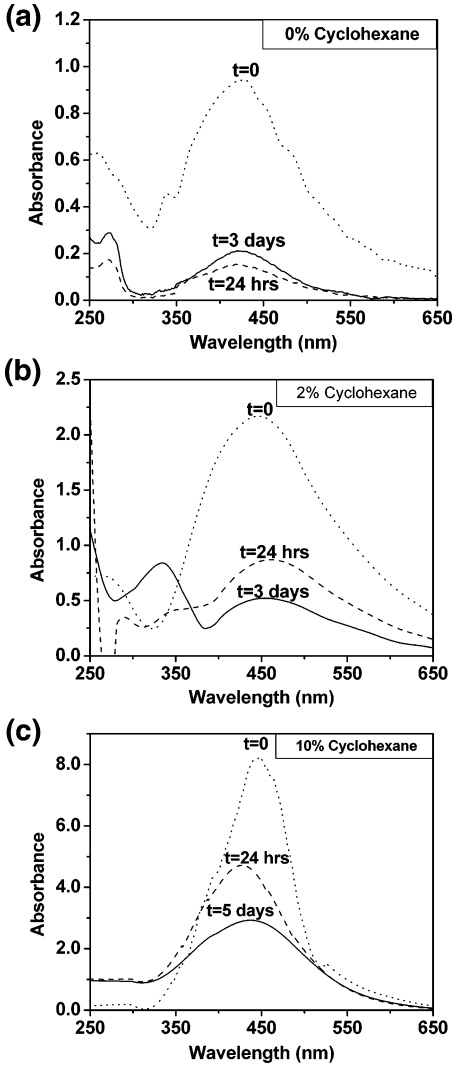

Figure 10. UV−vis spectra of isostearic acid coated silver nanoparticles synthesized in CO_2 at 295 K and 276 bar were taken at various time intervals with (a) no cosolvent, (b) 2% cyclohexane, and (c) 10% cyclohexane. The spectra have been scaled to have an absorbance of 0 at 700 nm for comparison. The dotted line corresponds to the initial absorbance, the dashed line to the absorbance after 24 h, and the solid line to the stable absorbance achieved after 3 days with 0 and 2% cyclohexane and after 5 days with 10% cyclohexane.

be synthesized in liquid CO_2 and then processed in the supercritical phase by a simple increase in temperature.

Effect of Time on Ag Nanoparticle Dispersion in CO_2. The influence of time on the dispersion of Ag nanoparticles in pure CO_2 and in each of the CO_2/cyclohexane mixtures was examined. UV−vis absorbance spectra were collected immediately after reduction of the Ag-AOT-TMH (defined as $t = 0$) and at regular time intervals until a stable dispersion was achieved. Immediately upon reduction, at $t = 0$, a strong UV−vis absorbance band with wavelength between 400 and 450 nm was observed in each of the CO_2/cylclohexane mixtures as shown in Figure 10. This strong absorbance at $t = 0$ corresponds to the rapid synthesis and dispersion of silver nanoparticles. In each CO_2/cyclohexane mixture, this absorbance band deceases in intensity with time, corresponding to the precipitation of those synthesized particles that could not be sterically stabilized (i.e. thermodynamically dispersed) in that particular solvent strength medium, again indicating that not all of the particles that were synthesized could be stably dispersed in the CO_2 mixtures. This UV−vis absorption intensity decreased with time until a stable dispersion was achieved in each solvent mixture after several days. In the case of neat CO_2, this absorption band rapidly dropped to a low absorbance value of ~0.2 absorbance units (au) after 24 h and remained effectively unchanged within 0.05 au after 3 days (within the experimental error of these measurements). It should be noted that while there was a significant decrease in absorption in neat CO_2 at steady state compared to that obtained immediately upon reduction, a fraction of the particles remain dispersed in neat CO_2 without the aid of fluorinated compounds or cosolvents. The addition of cyclohexane cosolvent resulted in both an increase in the initial absorbance intensity at $t = 0$ as well as an increase in the steady state absorbance corresponding to an increase in the concentration of Ag nanoparticles that were both synthesized and stably dispersed in these nonfluorinated CO_2 mixtures.

Conclusions

Silver nanoparticles capped with isostearic acid were synthesized and stabilized in a one-step process in pure CO_2 without the use of fluorinated surfactants or capping ligands. These dispersions are stabilized by molecular interactions between the ligand tails of isostearic acid and CO_2. The synthesis and dispersion of the isostearic acid capped Ag nanoparticles can be significantly enhanced by the addition of small amounts of cyclohexane cosolvent. Increases in pressure (or density) at a constant temperature also increase the concentration of dispersed particles. By a simple increase in temperature, the particles synthesized and dispersed in the liquid CO_2 phase can be processed in the supercritical phase without affecting their dispersion. This study indicates that nanoparticle processing in CO_2 solvent can be advanced without the need for environmentally persistent fluorinated compounds.

Acknowledgment. Auburn University would like to express its appreciation to the US DOE BES and the US DOE NETL for supporting this research through contracts DE-FG02-01ER15255 and DE-FG26-06NT42685, respectively. The University of Pittsburgh would like to express its appreciation to the US DOE NETL for supporting this research through Contract DE-FG26-04NT-15533. The authors would also like to thank Nissan Chemical for the gift of isostearic acid.

Supporting Information Available: We present the experimental procedure used to obtain the cloud point pressures of AOT-TMH in carbon dioxide and its variation as a function of temperature. This material is available free of charge via the Internet at http://pubs.acs.org.

References and Notes

(1) McHugh, M. A.; Krukonis, V. J. *Supercritical Fluid Extraction: Principles and Practice*, Butterworth-Heinemann: Boston, 1986.

(2) Esumi, K.; Sarashina, S.; Yoshimura, T. *Langmuir* **2004**, *20*, 5189.

(3) Shah, P. S.; Husain, S.; Johnston, K. P.; Korgel, B. A. *J. Phys. Chem. B* **2002**, *106*, 12178.

(4) Shah, P. S.; Husain, S.; Johnston, K. P.; Korgel, B. A. *J. Phys. Chem. B* **2001**, *105*, 9433.

(5) Shah, P. S.; Holmes, J. D.; Doty, R. C.; Johnston, K. P.; Korgel, B. A. *J. Am. Chem. Soc.* **2000**, *122*, 4245.

(6) Saunders: A. E.; Shah, P. S.; Park, E. J.; Lim, K. T.; Johnston, K. P.; Korgel, B. A. *J. Phys. Chem. B* **2004**, *108*, 15969.

(7) Ohde, H.; Hunt, F.; Wai, C. M. *Chem. Mater.* **2001**, *13*, 4130.

(8) McLeod, M. C.; McHenry, R. S.; Beckman, E. J.; Roberts, C. B. *J. Phys. Chem. B* **2003**, *107*, 2693.

(9) McLeod, M. C.; Gale, W. F.; Roberts, C. B. *Langmuir* **2004**, *20*, 7078.

(10) Fan, X.; McLeod, M. C.; Enick, R. M.; Roberts, C. B. *Ind. Eng. Chem. Res.* **2006**, *45*, 3343.

(11) Holmes, J. D.; Bhargava, P. A.; Korgel, B. A.; Johnston, K. P. *Langmuir* **1999**, *15*, 6613.
(12) Ji, M.; Chen, X.; Wai, C. M.; Fulton, J. L. *J. Am. Chem. Soc.* **1999**, *121*, 2631.
(13) Liu, J.; Raveendran, P.; Shervani, Z.; Ikushima, Y.; Hakuta, Y. *Chem.—Eur.* J. **2005**, *11*, 1854.
(14) Dong, X.; Potter, D.; Erkey, C. *Ind. Eng. Chem. Res.* **2002**, *41*, 4489.
(15) Yu, K. M. K.; Steele, A. M.; Zhu, J.; Fu, Q.; Tsang, S. C. *J. Mater. Chem.* **2003**, *13*, 130.
(16) Shah, P. S.; Holmes, J. D.; Johnston, K. P.; Korgel, B. A. *J. Phys. Chem. B* **2002**, *106*, 2545.
(17) Blackburn, J. M.; Long, D. P.; Cabanas, A.; Watkins, J. J. *Science (Washington, DC)* **2001**, *294*, 141.
(18) Watkins, J. J.; Blackburn, J. M.; McCarthy, T. J. *Chem. Mater.* **1999**, *11*, 213.
(19) McLeod, M. C.; Kitchens, C. L.; Roberts, C. B. *Langmuir* **2005**, *21*, 2414.
(20) Shah, P. S.; Novick, B. J.; Hwang, H. S.; Lim, K. T.; Carbonell, R. G.; Johnston, K. P.; Korgel, B. A. *Nano Lett.* **2003**, *3*, 1671.
(21) Johnston, K. P.; Harrison, K. L.; Clarke, M. J.; Howdle, S. M.; Heitz, M. P.; Bright, F. V.; Carlier, C.; Randolph, T. W. *Science* **1996**, *271*, 624.
(22) Hoefling, T. A.; Beitle, R. R.; Enick, R. M.; Beckman, E. J. *Fluid Phase Equilibria* **1993**, *83*, 203.
(23) Clarke, M. J.; Harrison, K. L.; Johnston, K. P.; Howdle, S. M. *J. Am. Chem. Soc.* **1997**, *119*, 6399.
(24) Shah, P. S.; Hanrath, T.; Johnston, K. P.; Korgel, B. A. *J. Phys. Chem. B* **2004**, *108*, 9574.
(25) Zhang, R.; Liu, J.; He, J.; Han, B.; Wu, W.; Jiang, T.; Liu, Z.; Du, J. *Chem.—Eur. J.* **2003**, *9*, 2167.
(26) da Rocha, S. R. P.; Dickson, J.; Cho, D.; Rossky, P. J.; Johnston, K. P. *Langmuir* **2003**, *19*, 3114.
(27) Eastoe, J.; Paul, A.; Nave, S.; Steytler, D. C.; Robinson, B. H.; Rumsey, E.; Thorpe, M.; Heenan, R. K. *J. Am. Chem. Soc.* **2001**, *123*, 988.
(28) Stone, M. T.; Smith, P. G., Jr.; da Rocha, S. R. P.; Rossky, P. J.; Johnston, K. P. *J. Phys. Chem. B* **2004**, *108*, 1962.
(29) Stone, M. T.; Da Rocha, S. R. P.; Rossky, P. J.; Johnston, K. P. *J. Phys. Chem. B* **2003**, *107*, 10185.
(30) Liu, J.; Han, B.; Li, G.; Zhang, X.; He, J.; Liu, Z. *Langmuir* **2001**, *17*, 8040.
(31) Ryoo, W.; Webber, S. E.; Johnston, K. P. *Ind. Eng. Chem. Res.* **2003**, *42*, 6348.
(32) Dickson, J. L.; Smith, P. G., Jr.; Dhanuka, V. V.; Srinivasan, V.; Stone, M. T.; Rossky, P. J.; Behles, J. A.; Keiper, J. S.; Xu, B.; Johnson, C.; DeSimone, J. M.; Johnston, K. P. *Ind. Eng. Chem. Res.* **2005**, *44*, 1370.
(33) Fan, X.; Potluri, V. K.; McLeod, M. C.; Wang, Y.; Liu, J.; Enick, R. M.; Hamilton, A. D.; Roberts, C. B.; Johnson, J. K.; Beckman, E. J. *J. Am. Chem. Soc.* **2005**, *127*, 11754.
(34) Brust, M.; Walker, M.; Bethell, D.; Schiffrin, D. J.; Whyman, R. *J. Chem. Soc., Chem. Commun.* **1994**, 801.
(35) Bell, P. W.; Anand, M.; Fan, X.; Enick, R. M.; Roberts, C. B. *Langmuir* **2005**, *21*, 11608.
(36) Nave, S.; Eastoe, J.; Penfold, J. *Langmuir* **2000**, *16*, 8733.
(37) Johnston, K. P.; Cho, D.; DaRocha, S. R. P.; Psathas, P. A.; Ryoo, W.; Webber, S. E.; Eastoe, J.; Dupont, A.; Steytler, D. C. *Langmuir* **2001**, *17*, 7191.
(38) Petit, C.; Lixon, P.; Pileni, M. P. *J. Phys. Chem.* **1993**, *97*, 12974.
(39) Bellamy, L. J. *The Infra-red Spectra of Complex Molecules*, 3rd ed.; John Wiley & Sons: New York, 1975.
(40) Wu, N.; Fu, L.; Su, M.; Aslam, M.; Wong, K. C.; Dravid, V. P. *Nano Lett.* **2004**, *4*, 383.
(41) Petroski, J.; El-Sayed, M. A. *J. Phys. Chem. A* **2003**, *107*, 8371.
(42) Nakamoto, K. *Infrared and Raman Spectra of Inorganic and Coordination Compounds*, 5th ed.; John Wiley & Sons: New York, 1997.
(43) Shafi, K. V. P. M.; Ulman, A.; Yan, X.; Yang, N.-L.; Estournes, C.; White, H.; Rafailovich, M. *Langmuir* **2001**, *17*, 5093.
(44) Ahn, S. J.; Son, D. H.; Kim, K. *J. Mol. Struct.* **1994**, *324*, 223.
(45) Tao, Y. T. *J. Am. Chem. Soc.* **1993**, *115*, 4350.
(46) Anand, M.; McLeod, M. C.; Bell, P. W.; Roberts, C. B. *J. Phys. Chem. B* **2005**, *109*, 22852.
(47) Kitchens, C. L.; McLeod, M. C.; Roberts, C. B. *J. Phys. Chem. B* **2003**, *107*, 11331.
(48) Kitchens, C. L.; Roberts, C. B. *Ind. Eng. Chem. Res.* **2004**, *43*, 6070.
(49) Cason, J. P.; Miller, M. E.; Thompson, J. B.; Roberts, C. B. *J. Phys. Chem. B* **2001**, *105*, 2297.
(50) Henglein, A.; Tausch-Treml, R. *J. Colloid Interface Sci.* **1981**, *80*, 84.
(51) Dimitrijevic, N. M.; Bartels, D. M.; Jonah, C. D.; Takahashi, K.; Rajh, T. *J. Phys. Chem. B* **2001**, *105*, 954.
(52) Ershov, B. G.; Henglein, A. *J. Phys. Chem. B* **1998**, *102*, 10663.
(53) Zhang, Z.; Patel, R. C.; Kothari, R.; Johnson, C. P.; Friberg, S. E.; Aikens, P. A. *J. Phys. Chem. B* **2000**, *104*, 1176.